scientific reports

Check for updates

OPEN

Optimizing the green synthesis of antibacterial TiO_2 - anatase phase nanoparticles derived from spinach leaf extract

Fatemeh Sheikh Ansari & Sara Daneshjou✉

Titanium dioxide nanoparticles, renowned for their abundance, non-toxicity, and stability, have emerged as indispensable components in various fields such as air purification, healthcare, and industrial processes. Their applications as photocatalysts and antibacterial agents are particularly prominent. The synthesis methods significantly influence the properties and subsequent applications of these nanoparticles. While several techniques exist, the biological approach using plant extracts offers advantages such as simplicity, biocompatibility, and cost-effectiveness. This study focused on the green synthesis of titanium dioxide nanoparticles utilizing spinach leaf extract. Within the scope of this investigation, the green synthesis of titanium dioxide nanoparticles through spinach leaf extract were synthesized and optimized, followed by a comprehensive examination of their morphological, structural, and chemical attributes with UV-visible spectroscopy, FTIR spectroscopy, XRD, FESEM, and EDX. The minimum inhibitory concentration (MIC) against E. coli and S. aureus was determined to evaluate their antibacterial potential. Optimal synthesis conditions were identified at 50 °C, using a 1/30 concentration and 20 ml of spinach leaf extract. Spherical anatase nanoparticles, ranging from 10 to 40 nm, were produced under these conditions. The change in the color of the extract, absorption at 247 nm, change and increase of the peak at 800 – 400 wavelengths, and the maximum intensity of X-ray diffraction at the angle of 25.367 with the crystal plane 101 were indications of the synthesis of these nanoparticles. Notably, the synthesized nanoparticles exhibited antibacterial activity with MIC values of 0.5 mg/ml against E. coli and 2 mg/ml against S. aureus. This research presents a novel, eco-friendly approach to synthesizing titanium dioxide nanoparticles with promising antibacterial properties.

Keywords Green synthesis, Optimization, Anatase, Spinach, Antibacterial nanoparticles

Titanium dioxide (TiO_2), alternatively referred to as titanium (IV) oxide or titania, is naturally found in mineral form. Following the groundbreaking research conducted by Fujishima and Honda in 1972, TiO_2-NPs have emerged as one of the most widely utilized metal oxides owing to their exceptional properties, including cost-effectiveness, abundance, Photocatalytic activity, and remarkable chemical, thermal, and biological stability. These nanoparticles, classified as non-hazardous by the United Nations, are produced on a large scale globally for various applications[1–4]. The intrinsic properties of nanoparticles, embodying dimensions, morphology, crystalline structure, dispersion, and specific surface area, exert direct control over the physical, chemical, and biological attributes that play a crucial role in determining their photocatalytic performance and ultimate application[5–7]. TiO_2 exhibits three distinct crystal phases, namely rutile, anatase, and brookite, each possessing unique characteristics, properties, and applications[8–10]. Among these phases, anatase is particularly well-known for its high photocatalytic activity when exposed to ultraviolet (UV) radiation[11]. This inherent trait enables anatase nanoparticles to exhibit remarkable antibacterial properties under UV irradiation. The shape and size of these nanoparticles, in conjunction with mechanical mechanisms, contribute to their ability to hinder bacterial growth or induce bactericidal effects. This effect is due to the indirect band gap of TiO_2, a type of semiconductor. When a photon excites an electron in the anatase lattice, the electron releases energy as a phonon (vibration) before reaching a higher energy level. Photons are electromagnetic waves, while phonons represent vibrations

Department of Nanobiotechnology, Faculty of Biological Science, Tarbiat Modares University, Tehran, Iran. ✉email: s.daneshjou@modares.ac.ir

within the crystal structure[6,12]. This process reduces the rate at which electron-hole pairs recombine, leading to more efficient oxidation and reduction reactions and preventing wasted energy as heat or light[13].

Nanoparticles can be effectively synthesized through targeted methods to attain distinctive structural, morphological, and property attributes that facilitate their ultimate application. The entirety of synthesis parameters, encompassing the characteristics of reactants, temperature, pH, concentration, and the like, play a direct role in determining the final properties of the resultant nanoparticles. Various techniques employed for nanoparticle production may impart advantages and disadvantages throughout the synthesis procedure. Nanoparticles are produced utilizing physical or chemical techniques as either top-down or bottom-up approaches[5,14,15]. In top-down methodologies, Miniaturizing the bulk materials to nanoscale dimensions induces surface imperfections, influencing the product's surface properties and physical characteristics. Conversely, the bottom-up approaches encompass building nanoparticles from individual atoms or molecules, employing chemical and physical processes. Regular techniques for synthesizing TiO_2 nanoparticles include sol-gel, hydrothermal, chemical vapor deposition, and simultaneous deposition[16,17]. However, these methods pose inherent difficulties concerning energy consumption, source utilization, and hazardous waste generation, presenting a formidable challenge in nanotechnology[18–21]. Developing novel, safe synthesis methodologies for nanomaterials thus emerges as a pressing imperative to bolster the demand for their application[22,23].

Within the purview of nanobiotechnology, biological materials are harnessed to fabricate nanomaterials with reduced toxicity and heightened biocompatibility, tailored for employment in sensitive domains such as biomedicine, person-centered medicine, environmental applications, biosensors, and agriculture[24–27]. Since the 19th century, scientists have acknowledged the inherent capacity of biological organisms, particularly plants, to degrade metal precursors[28]. The preference for plants arises from their widespread accessibility and the potential for large-scale production[28]. In contrast to microbes, plants exhibit a shorter time frame for the reduction of metal ions and do not necessitate sterile conditions, complex intracellular culturing and synthesis procedures, purification steps, expensive equipment, or specialized labor, While plant-based synthesis may have slower production rates for large-scale applications, it compensates with these advantages[29,30]. Notably, the employment of plant extracts in laboratory settings has garnered attention due to the expeditious production kinetics and streamlined synthesis methodology[31]. Previous studies have employed various plant components to prepare such extracts. Phytochemical constituents present within plants Influence the nanoparticle fabrication process, conclusive applications of synthesized nanoparticles, and augment the appeal of green synthesis methods[10,32]. For instance, phytochemicals involved in the reduction of titanium ions for TiO_2 nanoparticle synthesis can enhance the photocatalytic properties of the resultant nanoparticles through their active participation in oxidation and reduction processes[32,33]. Table 1 provides exemplary green TiO_2 synthesis employing plant leaf extracts.

Spinach, an annual or rarely biennial vegetable belonging to the *Amaranthaceae* family, is believed to have originated from Central Asia, particularly Iran, before being introduced to Spain in the 14th century and its Latin name, spinach, derives from the word Hispania, signifying Spain[44]. Spinach holds significant dietary importance due to its low-calorie content, high nutritional value, having a lot of vitamins (such as vitamin K and carotene, a precursor to vitamin A), and minerals like iron and calcium. Moreover, spinach contains phytonutrients, including phenols, flavonoids, and phlobatanins, which possess noteworthy medicinal properties[30,45,46]. However, it is crucial to note that the quantity of these metabolites extracted from each plant depends on factors such as plant species, plant parts, and the extraction method employed[45,47,48]. The interconnection between spinach and nanotechnology manifests in two distinct ways. Firstly, studies explore the impact of various nanoparticles on spinach plants, including their effects on plant hormones and growth[49]. Secondly, the principles of green chemistry are employed to synthesize diverse nanoparticles using spinach as a starting material. Given the significantly higher iron content in spinach compared to other plants, researchers view the synthesis of iron oxide from spinach as an economically viable and environmentally friendly approach[29,50–53]. Additionally,

Plant	Characterization	Size (nm)	Shape	Aim	Ref
Morus nigra	FTIR, XRD, SEM, Raman	0.17	Spherical	Negligible toxic hemolytic effects, little inhibition of Staphylococcus aureus and Proteus Mirabilis bacteria as compared to ciprofloxacin	34
Carthamus tinctorius L.	XRD, SEM, EDX	47	Spherical	Fuel blends for diesel/biodiesel/NP in a single-cylinder CI engine	35
Phyllanthus acidus	XRD, FTIR, FESEM- EDX, TEM, BET	20–40	Spherical	Performance of heavy metal adsorption of TiO_2 nanoparticles	36
Gossypiumarboretum	XRD, SEM, TEM	60	Spherical	The attractive catalyst for biodiesel production from Gossypium seed oil	37
Tulbhagia violacea	UV-Vis, FTIR, XRD, SEM, EDX, TEM	-	Spherical and rectangular	Antioxidant and anticancer activities	38
Calotropis gigantea	UV-Vis, XRD, FTIR, TEM	12.16	Spherical	Photocatalytic and photovoltaic applications	35,39
grape	UV-Vis, BET, FTIR, XRD, SEM-EDX	44.37	Spherical	Photocatalytic degradation of ibuprofen from aqueous solution	40
Annona muricata L.	UV-Vis, FTIR, XRD, SEM, EDX, TEM, XRF, confocal microscope	13.41	Spherical	Antioxidant and photocatalytic activity	41
Beta vulgaris	FTIR, XRD, FESEM, HRTEM, SEAD, BET, Raman	12	Spherical	The aqueous binder-based anode-derived particles for lithium-ion cells	42
Amaranthus Tricolor L.	UV-Vis, FTIR, XRD, SEM, EDX, TEM, TG-DTA	77–90	Spherical	Photocatalytic of methylene blue degradation	43

Table 1. Green TiO_2 synthesis employing plant extracts.

spinach leaf extracts have been utilized to fabricate nanoparticles such as silver[54], zinc oxide[30,32], copper[55], and cobalt[15]. In all these studies, spinach extract has demonstrated favorable regenerative properties.

This study explores the biosynthesis of titanium dioxide nanoparticles using spinach leaf extract, emphasizing the value of green synthesis in light of the increasing plant biodiversity. The research addresses the challenges of producing nanoparticles with the desired size, phase, and properties while minimizing costs and resource use, especially for large-scale applications. Given Iran's extensive spinach cultivation and the plant's abundant reducing agents, we aim to efficiently reduce metal ions into nanoscale titanium dioxide particles, specifically the anatase phase. Anatase's exceptional photocatalytic properties are valuable across biomedicine, drug delivery, agriculture, and environmental science. By demonstrating the antimicrobial capabilities of our synthesized nanoparticles, we contribute a novel dimension to the expanding field of biological metal nanoparticle applications.

Experimental

Materials

Titanium oxysulfate (Sigma-Aldrich)-sodium hydroxide (Dr. Mojalli) - Folded filter paper (Whatman) - Lb broth culture medium (Merk) - *Staphylococcus aureus* [S. aureus] (PTCC 1337) and *Escherichia coli* [E. coli] (ATCC 25922).

Extract preparation

Spinach leaves were harvested from spherical and planar seed varieties cultivated on a Tehran-Qalenou farm. Subsequently, Fresh leaves were detached from the stems and subjected to a thorough washing procedure involving three rinses with tap water to eliminate dust particles, followed by a final rinse with distilled water to ensure optimal cleanliness. After removing excess moisture from the leaves, they were chopped and subjected to a five-day drying process in a room devoid of direct sunlight. The resulting dried leaves were then pulverized into a fine powder using a domestic grinding apparatus. Two distinct samples of spinach leaf extract were prepared by combining 1 gram of spinach powder with 30 and 10 ml of boiling deionized water, then stirred at 50 °C for 30 min before cooling. The extract was filtered using filter paper and a 0.22-micron filter. Figure 1 illustrates this process.

TiO_2 NPs synthesis

To optimize the synthesis, from each extract, volumes of 500 and 1000 µl, 10, 20, and 40 milliliters, were separately transferred to falcon tubes. Subsequently, 200 µl of a 0.5 M $TiOSO_4$ solution was added to each sample. Samples were agitated at 70 °C, 50 °C, and room temperature for 15 min. 0.1 M sodium hydroxide was added to each sample to achieve a pH of 8. The samples were again transferred to the incubator with the same temperature conditions for 15 h. Then, they were left at room temperature for five days, allowing for the completion of the synthesis process and the subsequent precipitation of titanium dioxide nanoparticles. The resulting precipitates were Centrifuged at 25 °C for 20 min at 9000 rpm. The supernatant was discarded, and the sediments were washed with distilled water to eliminate residual impurities. The sediments were centrifuged once again under the same conditions. The sediment was resuspended in 20 ml of distilled water, transferred to glass plates, and

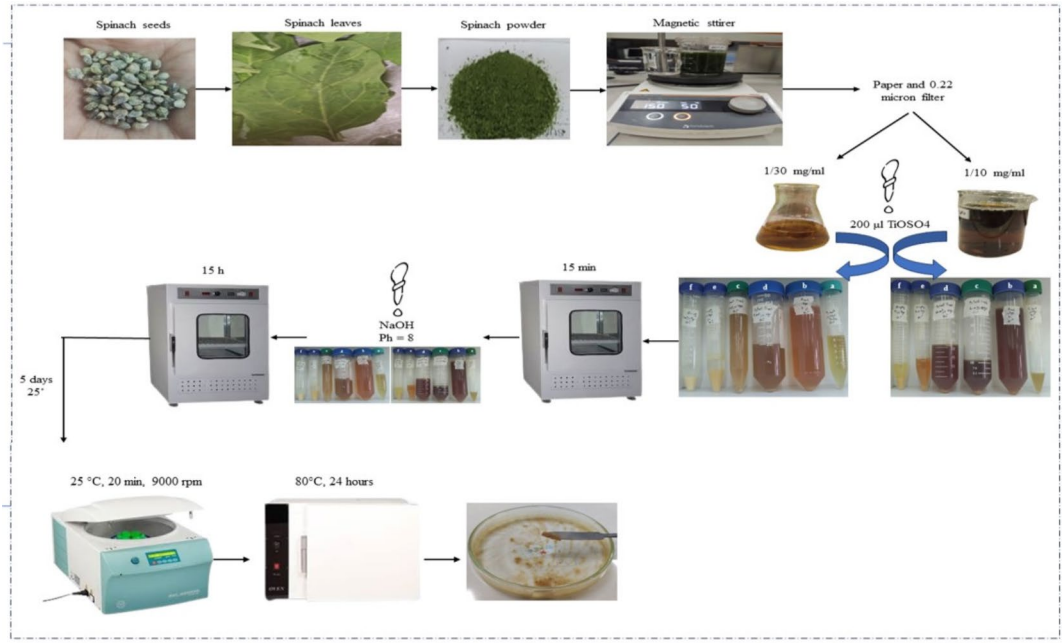

Fig. 1. Schematic of extract preparation and TiO_2 NPs synthesis.

	C1			C2		
V1	V1 C1 T1	V1 C1 T2	V1 C1 T3	V1 C2 T1	V1 C2 T2	V1 C2 T3
V2	V2 C1 T1	V2 C1 T2	V2 C1 T3	V2 C2 T1	V2 C2 T2	V2 C2 T3
V3	V3 C1 T1	V3 C1 T2	V3 C1 T3	V3 C2 T1	V3 C2 T2	V3 C2 T3
V4	V4 C1 T1	V4 C1 T2	V4 C1 T3	V4 C2 T1	V4 C2 T1	V4 C2 T3
V5	V5 C1 T1	V5 C1 T2	V5 C1 T3	V5 C2 T1	V5 C2 T1	V5 C2 T3
	T1	T2	T3	T1	T2	T3

Table 2. Sample codes based on the investigated parameters. T: temperatures T1 = 25 °C, T2 = 50 °C, T3 = 70 °C C: extract concentrations C1 = 1/30 C2 = 1/10 V: extract volumes V1 = 500 µl, V2 = 1000 µl, V3 = 10 ml, V4 = 20 ml, V5 = 40 ml

samples	pH after adding $TiOSO_4$ (pH = 2)	pH after adding NaOH
V1	3	8
V2	3	8
V3	5	8
V4	5	8
V5	> 6	8

Table 3. pH changes during the synthesis of nanoparticles.

dried in an oven at 80 °C for 24 h. Figure 1 outlines the synthesis process, and Table 2 details the sample variations based on temperature, extract concentration, and volume.

Characterization

The present study aims to investigate the characterization of green nanoparticles generated using various analytical techniques, including ultraviolet-visible spectroscopy (lambda25), Fourier transform infrared spectroscopy (PerkinElmer - Spctrumtwo), x-ray diffraction (Panalytical - X'pert pro), field emission scanning electron microscopy, and diffuse reflectance spectroscopy (ZEISS - Sigma vp). The primary objective is to identify the optimal synthesis conditions that facilitate the attainment of the pure phase of anatase, thereby enabling an in-depth assessment of its properties.

Investigation of antibacterial properties

Cultivating bacteria

Initially, individual strains of S. aureus as a Gram-positive bacteria and E. coli as a Gram-negative bacteria were thawed from long-term storage in a 50% glycerol solution maintained at -80 °C. 10 µl of each bacterial suspension was inoculated into 10 ml of autoclaved Lb broth medium and incubated at 37 °C for 16 h to ensure the attainment of a bacterial suspension exhibiting a turbidity level equivalent to half of the McFarland standard, specifically denoted as 1.5×10^8 cells/ml.

Minimum inhibitory concentration test

The Minimum Inhibitory Concentration (MIC) is the lowest antimicrobial concentration preventing microbial growth after incubation[56]. The diagnostic index for this test is the light absorption by the microorganisms, which is quantified using either a spectrophotometer or a microplate reader. In the present research, the MIC values for the synthesized TiO2 nanoparticles against E. coli and S. aureus strains were determined using the broth microdilution method. 50µL of nanoparticle dilutions (2, 1, 0.5, 0.25, and 0.125 mg/ml) were prepared and added to a 96-well plate. Furthermore, 50µL of 100 times 100 times bacterial suspensions (1.5 × 106 cells/ml) were inoculated into the corresponding wells. Control wells contained spinach extract or deionized water with bacteria. The absorbance of the samples was measured at a wavelength of 600 nm using a microplate reader (Biotek-Uqant). Following a 24-hour incubation at 37 °C and a shaker speed of 120 rpm, the absorbance was measured again at the same wavelength. This sequential measurement allowed for rating any alterations in absorbance during the incubation period, thereby providing valuable insights into the antibacterial behavior of the samples under investigation. It is worth noting that although ultraviolet (UV) radiation is known to enhance the antibacterial properties of TiO2, all experimental procedures were conducted in the absence of light[33,57].

Results

Both spinach extracts exhibited a neutral pH of 7. After adding acidic 0.5 M $TiOSO_4$ salt solution (pH 2), the pH stabilized at 3 for 500 and 1000 µl samples, 5 for 10 and 20 ml samples, and 6 for 40 ml samples, regardless of temperature. The pH was adjusted to 8 with 0.1 M sodium hydroxide following a 15-minute agitation period. Table 3 summarizes these pH changes.

An immediate color change upon salt addition confirmed in-situ nanoparticle formation. While the same color variations occurred across temperatures, only the 50 °C samples are shown in Fig. 2. Following synthesis,

samples were prepared for characterization. Optimal parameters were determined through sequential sample elimination based on characterization results.

UV-visible spectroscopy

This study utilized the colloidal nanoparticle solution before drying. Figure 2 presents the absorption spectra of extracts at 255–290 and 330–390 nm and sample spectra within the 240–280 nm range. V2 samples exhibited a significantly higher peak intensity, while V2C2T3 showed the broadest peak from 240 to 314 nm. Samples with low peak intensity or no peaks in the specified range were discarded. V3C1T1 and V4C2T1 were removed due to low peak intensity, while V1C1T1, V1C1T3, V4C1T3, and V4C2T3 were excluded for lacking the desired peak. Due to overlapping peaks, T2 samples were retained for further analysis.

FTIR spectroscopy

The selected samples from each extract were centrifuged, washed, and dried to produce a powder. Potassium bromide (KBr) was mixed with the powders to create a tablet for analysis. Infrared radiation was used to measure the resulting vibrations, and the obtained spectra were compared to those of the respective extracts within the 400–4000 cm^{-1} wavenumber range (Fig. 3). Since metal-oxygen bond peaks typically reside in the fingerprint region, the analysis focused on the 400–800 cm^{-1} range. Among T1 samples, V5 samples from both extracts were excluded due to lacking distinct peaks compared to their respective extracts. Specifically, within the C1T1 samples, only the V2 sample exhibited the desired peak with an acceptable intensity. For the C1T3 samples, V2 and V5 were eliminated as V3 displayed a more prominent, competing peak. Once again, due to the proximity of the peaks, no elimination was carried out for the T2 samples.

XRD

The evaluation of x-ray diffraction with diffraction angles ranging from $2\theta = 10°$ to 90° was conducted on the selected powdered samples, as well as on the synthesized TiO2 nanoparticles, using the standard data provided by the [2003 JCPDS-International Center for Diffraction Data-reserved PCPDFWIN v.24]. This analysis confirmed the synthesis of TiO2 nanoparticles and facilitated the identification of crystal phases. The results presented in Fig. 4 revealed that all T1 samples exhibited a diffraction maximum at $2\theta = 25.33°$and the lattice plane 101, corresponding to the standard tetragonal crystal state and the anatase phase. However, for samples V2C1T2, V2C2T2, V5C1T2, V5C2T2, and V3C2T2, no crystalline phase of titanium dioxide was observed. Notably, the diffraction pattern in Fig. 4 indicated the presence of the rutile phase in sample V4C2T2. On the other hand, the remaining T2 samples displayed the anatase crystal phase, and their patterns closely resembled those of the T1 samples. The sample V3C2T3, exhibited the rutile phase, while the other two samples were amorphous at T3.

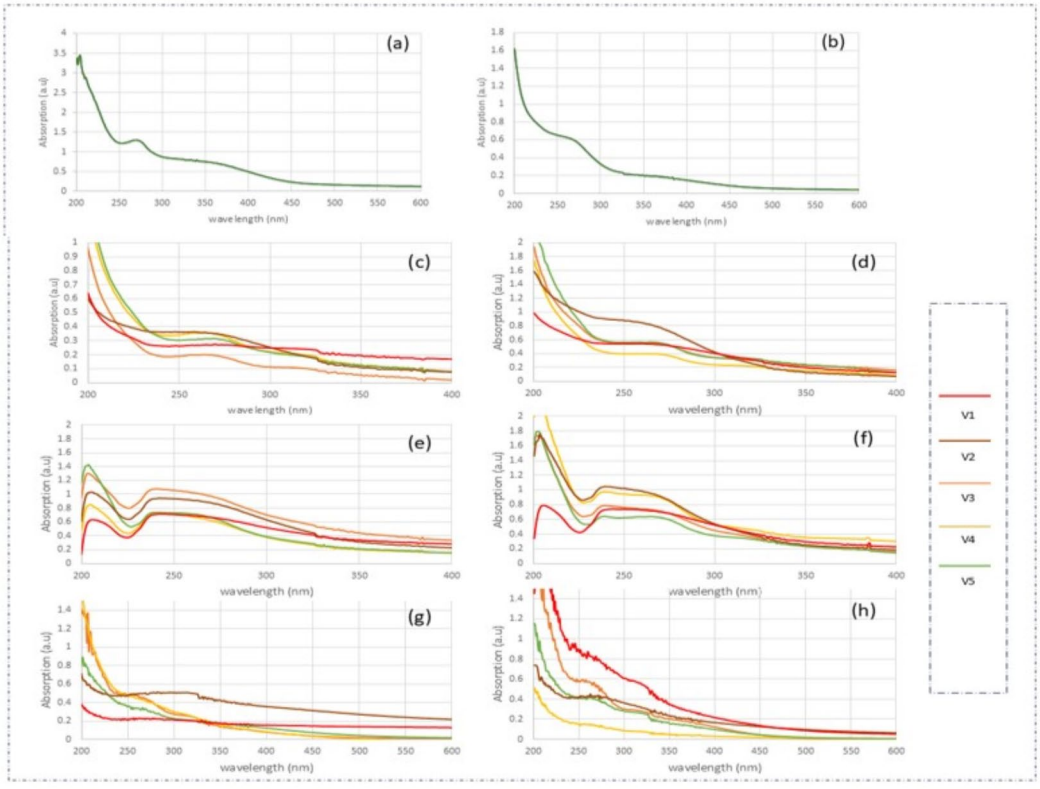

Fig. 2. Absorption spectrum of spinach leaf extract (**a**) C1 (**b**) C2 - Absorption spectrum of samples (**c**) C2T1 (**d**) C1T1 (**e**) C2T2 (**f**) C1T2 (**g**) C2T3 (**h**) C1T3.

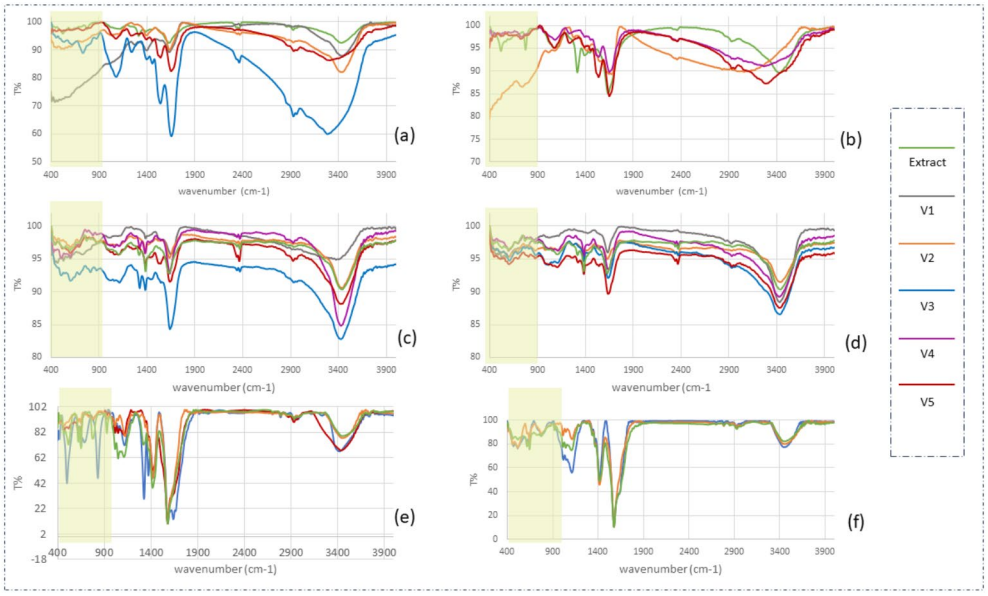

Fig. 3. FTIR spectrum of (**a**) C2T1 (**b**) C1T1 (**c**) C2T2 (**d**) C1T2 (**e**) C2T3 (**f**) C1T3.

This suggests that the desired formation of titanium dioxide was less favorable at this particular temperature, indicating its limited suitability for achieving the desired crystalline structure. All the results are also summarized in Table 4.

FESEM and EDX spectroscopy

Nanoparticle deposition involved drying an aqueous solution onto a slide, imaging the surface under a microscope, and determining particle size (up to 200 nm) using electron bombardment. In addition, EDX spectroscopy is a supplementary technique in conjunction with FESEM imaging (Fig. 5). Particle sizes range from 10 to 70 nm. Although Fig. 5-e shows a selected rutile sample with an undesirable size, it was included to contrast with anatase in microbial susceptibility testing. Larger, aggregated samples were excluded due to prior expectations.

FESEM emits primary electrons that eject secondary electrons from the sample surface. These electrons are detected, and their pattern reveals surface topography[58]. Particle size was determined using image processing software (ImageJ) on FESEM images, following methods outlined in Wei et al.[59], Shahin Lefteh et al.[60], Velayutham et al.[61], Mobeen Amanulla[62], Rajendhiran et al.[63], and Aravind et al.[64]. Statistical analysis of multiple regions is crucial for accurate results. Figure 6 presents the particle size distribution for an optimal sample. The EDX results demonstrate the presence of titanium dioxide nanoparticles, as confirmed by the quantitative and qualitative detection of titanium atoms and oxygen. Moreover, the spectroscopy reveals the presence of other elements derived from biosynthesis on the nanoparticles.

Antibacterial properties

Out of the 24 cases, four samples exhibited desirable results and anatase phases across all employed methods.

A summary of these characterization techniques and removals during different stages is shown in Fig. 7.

These samples with a rutile sample denoted as V4C2T2 underwent a liquid microdilution test to determine their minimum inhibitory concentrations (MIC). For this purpose, a 16-hour cultivation of Gram-positive bacteria (S. aureus) and Gram-negative bacteria (E. coli) was conducted in a liquid medium known as Lb broth to obtain a bacterial concentration equivalent to half of the McFarland standard.

Initially, a 2 mg/ml dilution of each sample was prepared for inter-sample comparison. 50 µl of each sample was added to separate wells of a 96-well plate and incubated with 50 µl of diluted bacterial suspension for 24 h with shaking. Deionized water and spinach leaf extract served as negative controls. Bacterial absorbance was measured using a microplate reader before and after incubation, and the results were compared to the control. The findings are summarized as follows:

All samples, except the V1C1T1 sample, demonstrated the ability to inhibit the growth of S. aureus bacteria. Among them, only the anatase V4C1T2 sample exhibited an impact on E. coli bacteria. Notably, the rutile sample exhibited weaker antibacterial properties than the anatase sample. Furthermore, no antibacterial activity was observed for the spinach extract.

Subsequently, another experiment was conducted with different dilutions for anatase (V4C1T2) to determine the minimum inhibitory concentration (MIC) value. The concentrations of 0.125, 0.25, 0.5, 1, and 2 mg/ml were prepared. The steps were repeated for new concentrations. Figure 8 illustrates the absorbance measurements before and after incubation. The results were reproducible for a dilution of 2 mg/ml. Analysis of the absorbance of E. coli bacteria indicated a significant decrease in absorbance for both the 2 and 1 mg/ml dilutions of anatase

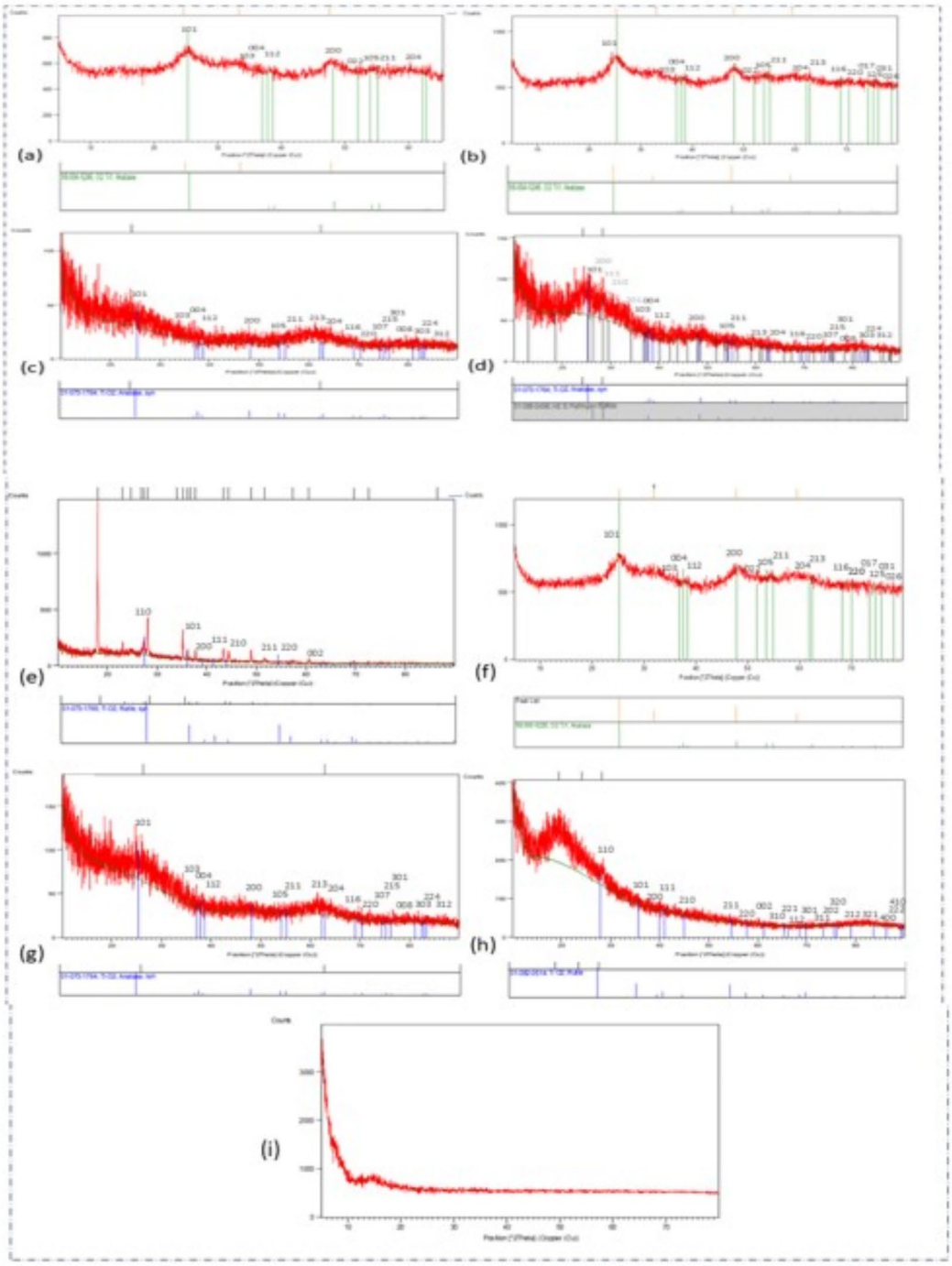

Fig. 4. XRD patterns of selected particles (**a**) V1C2T1 (**b**) V2C1T1 (**c**) V1C2T2 (**d**) V1C1T2 (**e**) V4C2T2 (**f**) V4C1T2 (**g**) V3C1T2 (**h**) V3C2T3 (**i**) amorph pattern.

nanoparticles following the incubation. Although the previous dilution (0.5 mg/ml) did not exhibit significant bacterial growth and increase in absorbance, it was considered the minimum inhibitory concentration. Evaluation of S. aureus bacteria uptake corroborated the observations from the preceding experiment, identifying the 2 mg/ml dilution as the minimum inhibitory concentration.

A comprehensive analysis of the selected anatase sample

A complete analysis was conducted on the chosen anatase sample. The UV-VIS absorption spectrum, FTIR spectrum, and XRD pattern are presented in Fig. 6. The crystallite size, calculated from the X-ray peaks using Scherer's equation (Table 5), is approximately 30 nm. The UV-VIS spectrum revealed a λmax value of 250 nm, indicative of the absorption behavior of anatase. In the FTIR spectrum of anatase nanoparticles, a

		Anatase	Rutile	Amorph
C1	T1	V2	-	-
	T2	V1 V3 V4	-	V2 V5
	T3	-	-	V1 V3
C2	T1	V1		
	T2	V1	V4	V2 V3 V5
	T3	-	V3	-

Table 4. XRD results of selected samples.

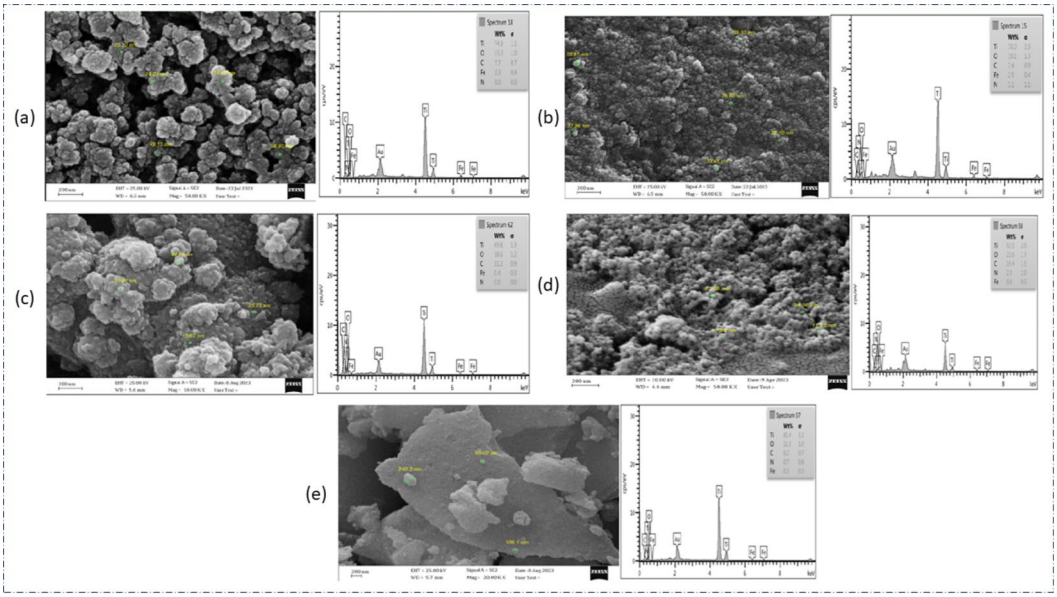

Fig. 5. FESEM and EDX of selected particles (**a**) V1C2T1 (**b**) V2C1T1 (**c**) V1C1T2 (**d**) V4C1T2 (**e**) V4C2T2.

distinctive and robust peak was observed at 3424.52 cm^{-1}, alongside several prominent peaks at 1638.05 cm^{-1}, 1383.75 cm^{-1}, and 596.79 cm^{-1}. Additional noteworthy peaks were identified at 1113.99 cm^{-1}, with weaker peaks at 2929.29 cm^{-1}, 2370.7 cm-1, 874.03 cm^{-1}, and 448.47 cm^{-1}, located between them. Other significant peaks were placed at 1634.16 cm^{-1} and 530.26 cm^{-1}, while two weaker peaks were evident at 2924.45 cm^{-1} and 1061.08 cm^{-1}. The peak at 596.79 cm^{-1} can be attributed to Ti-O vibrations of anatase.

Discussion

In recent decades, there has been an increase in research focused on biological synthesis, particularly in nanoparticle fabrication. Plant species show considerable diversity and ability to produce nanoparticles with distinct shapes, sizes, and properties. However, using spinach leaves for titanium dioxide nanoparticle synthesis and optimization has not been pursued until now.

Spinach (Spinacia oleracea) is known by various types, including Savoy, Semi-Savoy, Flat/smooth leaf spinach, etc.44For this project, spinach was cultivated from bladeless seeds. The nutritional and therapeutic value of spinach is widely recognized, owing to its rich content of organic and mineral nutrients. The phytochemical composition of a plant directly influences the properties of the nanoparticles synthesized using that plant, thereby determining their potential applications. This research is inspired by the studies of B. Fayyaz et al.[53] and A. Djouad[32] using spinach plant extract and employed 0.22-micron filters to remove impurities and microorganisms, similar to other studies[1,65–68] These physical barriers serve to obtain a relatively pure extract for the synthesis of titanium dioxide nanoparticles. However, the quantitative evaluation of the effectiveness of this filtration method has not been reported in their studies. Titanium dioxide nanoparticles possess advantageous characteristics, including low toxicity, high biocompatibility, and affordability, which make them highly appealing for investigation and utilization across diverse fields. The biological synthesis of these nanoparticles using spinach as a precursor offers desirable benefits and properties. The synthesis of these nanoparticles utilizing titanium oxysulfate ($TiOSO_4$) was based on the work of S. Subhapriya[69].

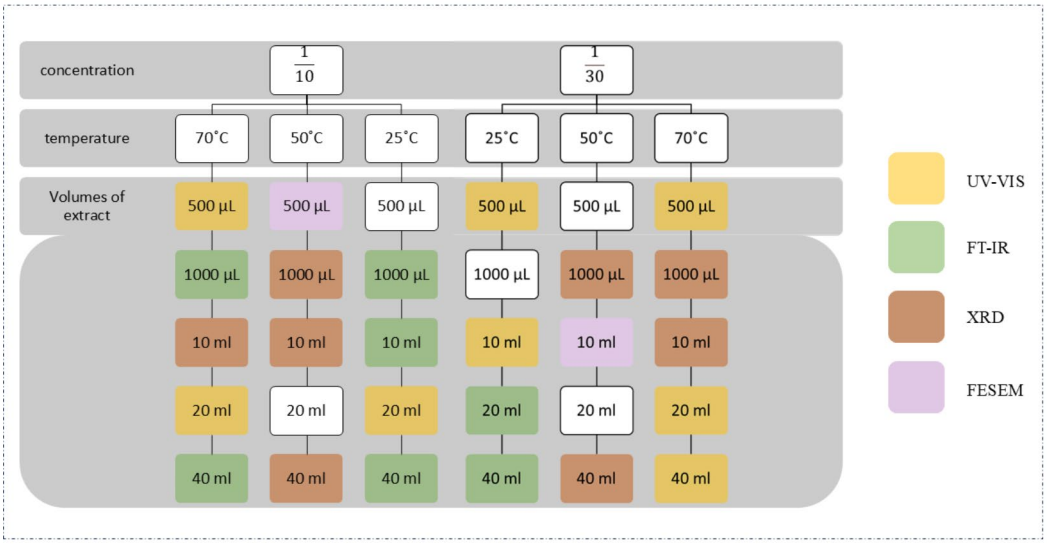

Fig. 6. Complete analysis of anatase (**a**) UV-VIS spectrum (**b**) FTIR spectrum of spinach and anatase comparison (**c**) FTIR spectrum of anatase (**d**) Anatase crystal pattern and its parameters (**e**) FESEM and EDX (**f**) Particle distribution diagram.

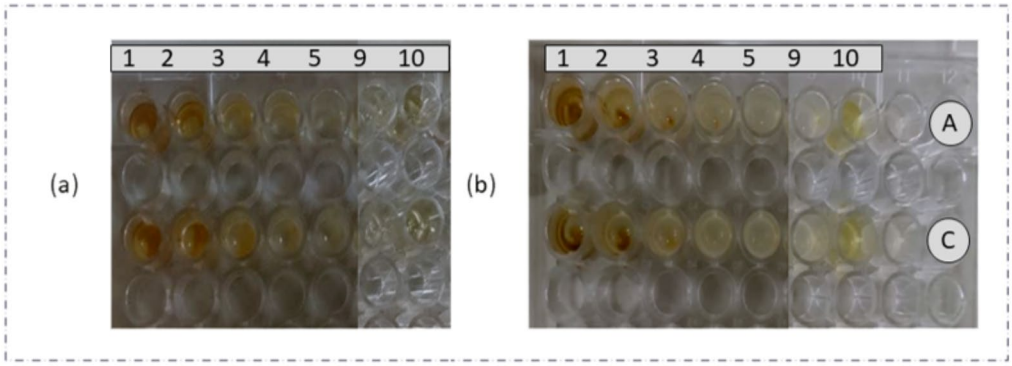

Fig. 7. A summary of this characterization and removals during different stages (Each color represents the deletion of that sample with the determined methods.)

In nature, titanium dioxide has three phases: anatase, brookite, and rutile. However, in laboratory settings, these phases can be synthesized. In this research, the focus is on obtaining the anatase phase due to its superior photocatalytic properties.

The optimization of green synthesis methods for titanium dioxide nanoparticles has received limited attention in previous research. A study exploring the optimization of pH for nanoparticle synthesis using chamomile flower extract revealed that an increase in pH corresponded to an increase in particle size[16].

This research focuses on determining the optimal temperature, extract concentration, and required extract volume with a fixed amount of salt to achieve the pure anatase phase. Additionally, another study investigated the synthesis of titanium dioxide nanoparticles using the E. cinerea plant, exploring the effects of pH, extract concentration, and temperature. The optimal parameters identified in this study were a temperature of 25° C, an extract concentration of 2/10, and pH 9. The XRD pattern analysis indicated that the synthesized nanoparticles exhibited the rutile form, with maximum intensity at a diffraction angle of 27.3°[70]. A comparison of optimization parameters from this research and previous studies is presented in Table 6.

The pH parameter significantly influences the crystalline structure of nanoparticles in the final product. Extensive research has indicated that the formation of the rutile form is predominantly under highly acidic conditions, while alkaline conditions favor the anatase form. Under weakly acidic conditions, the brookite form tends to be synthesized[12]. Consequently, the present study selected a pH of 8 as the fixed alkaline condition.

A visible color change in the extract confirmed the successful synthesis of titanium dioxide nanoparticles. Previous research by M. Narayanan et al.[74] and S. Vembu et al.[75] reported color variations, including red or gray,

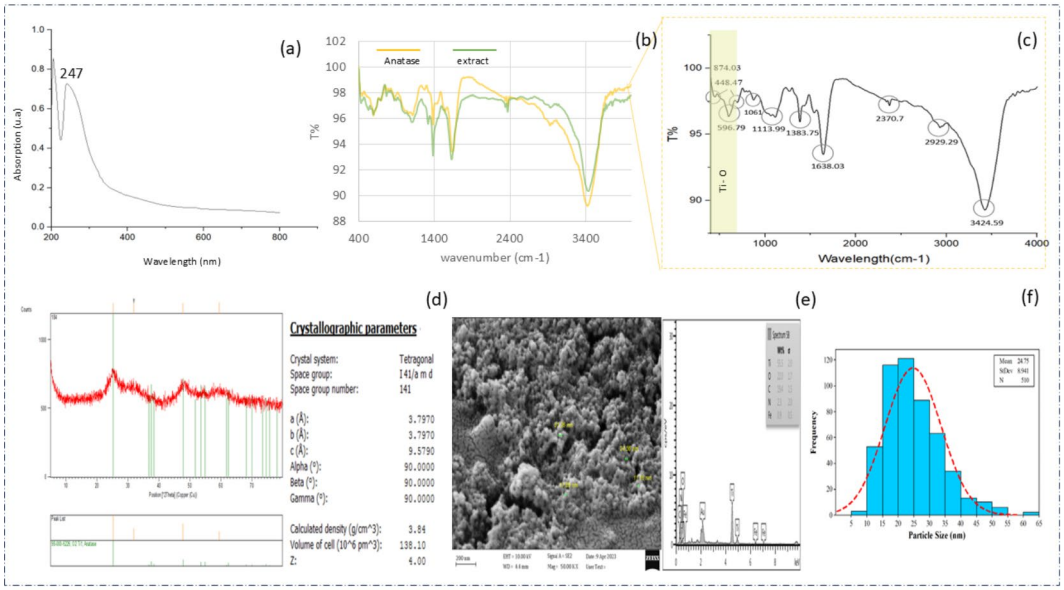

Fig. 8. Broth microdilution of anatase sample (V4C1T2) (**a**) before incubation (**b**) after incubation (Wells 1–5 related to samples 2, 1, 0.5, 0.25, and 0.125 mg. Also, numbers 9 and 10 are related to water and spinach extract, respectively. Row A is related to E.coli and C is related to S.aureus.)

Pos.[°2Th.]	Height [cts]	FWHM Left[°2Th.]	d-spacing [Å]	Int. [%]
25.184310	115.234200	3.517126	3.53333	100.00
31.882170	52.486550	8.543439	2.80467	45.55
47.741840	73.360430	2.808289	1.90349	63.66
59.506420	38.715260	7.152272	1.55219	33.60

Table 5. Calculation of crystallite size from the subsequent peaks.

Plant	Parameter	Optimized	Result	Ref
E. cinerea	pH temperature extract concentration	9 25 °C 2/10	Rutile	[70]
chamomile	↑pH		↑particle size	[16]
C. citratus	pH	10	Anatase	[71]
C. aurantium	pH	8	Anatase	[72]
L. acidissima	pH	8	Anatase	[73]
spinach	pH temperature extract concentration extract volume	8 50 °C 1/30 20 ml	Anatase	This project

Table 6. Optimized parameters for the synthesis of TiO_2. ↑ : increase

following nanoparticle formation. These color changes can occur immediately upon precursor salt addition or after a specific incubation period[76]. M. Shahin Lafteh et al. documented the synthesis of titanium dioxide nanoparticles employing Iranian mangrove leaves, which induced a light brown coloration in the plant extract after a delay of 10 min[60]. This coloration closely resembled the colloidal solution of anatase employed in this study.

Spinach contains several active antioxidant flavonoids. Hnin Yu et al. confirmed and quantified these complex polyphenols in spinach[77]. Flavonoids can be categorized into various groups based on the functional groups present on the flavonoid ring. Flavonoids are classified based on their functional groups. Quercetin, a prominent flavonoid, is abundant in various vegetables, among which onions and spinach are the richest sources[78]. Phenolic compounds exhibit distinct absorption spectra with two peaks. The first one, around 280 nm, originates from the aromatic ring, and the second one, occurring at longer wavelengths (300–360 nm), is equally significant.

Interestingly, Solovchenko's study[79] highlighted a peak related to quercetin—a well-known flavonoid—in a manner almost identical to the peak obtained from our spinach leaf extract. However, it's essential to note that boiling after storing spinach leaf powder at 4 °C can lead to the breakdown of complex structures into simpler phenols[80]. The absence of the second peak in the synthesized samples may be attributed to thermal effects and the regenerative properties of certain substances used during the synthesis process.

UV-VIS spectroscopy (200–800 nm) is commonly used to characterize nanoparticle-light interactions and estimate particle size. An absorption peak closer to 200 nm generally indicates smaller nanoparticles. This aligns with J. Doak et al.'s findings, where strong absorption of gold nanoparticles at longer wavelengths suggested larger particles within their size distribution[81]. Additionally, the peak less than 300 nm closely resembled the peak exhibited by anatase nanoparticles synthesized using S. cumini extract. The light brown color of the nanoparticle colloid in this study further reinforces this similarity[82].

The color observed in the synthesis solution persisted through separation and drying, resulting in colored nanoparticle powders. Typically white, the nanoparticles likely acquired their color from adsorbed spinach metabolites. Spinach contains carotene, a pigment that imparts orange hues to certain plants[83]. The presence of these pigments during synthesis contributed to the production of colored powders. Notably, reducing the extract volume decreased the concentration of coloring agents, resulting in near-white powders. Consequently, nanoparticles synthesized using extract, particularly at volumes of 500 and 1000 µl, exhibit a cream-like color, while anatase nanoparticles synthesized using 20 ml of extract retain their light brown color. Notably, the generation of titanium dioxide powder and colored deposits has been reported not only in this project but also in the studies conducted by S. Balaji et al.[84] and A. Mobeen Amanulla[62].

Numerous investigations have been conducted on the anatase phase, and the diffraction angles reported in these studies exhibit a similar pattern to the anatase diffraction angles observed in the present. The morphology of the synthesized titanium nanoparticles, as examined through scanning electron microscopy (SEM) or field emission scanning electron microscopy (FESEM), has predominantly displayed a spherical shape in previous studies[2,63,84,85]. Nevertheless, alternative shapes, including triangular structures[62], cubic forms[86], and flower-like particles[87], have also been documented. Also, in addition to morphology, the particle size can be estimated. The particle size distribution estimated from this technique is consistent with the size calculated by XRD.

Green synthesis methods utilize various products, by-products, and discarded components of living organisms to fabricate nanoparticles. Eggshells serve a similar function to spinach in reducing the $TiOSO_4$ precursor salt to fabricate spherical anatase nanoparticles with an average size of 38 nm. These nanoparticles exhibit maximum absorption at 382 nm, suggesting that the ultraviolet absorption spectrum can indicate the photocatalytic performance of the particles under UV light[88].

Another case is to investigate the surface properties of synthesized titanium dioxide nanoparticles. Phytochemicals found in plants play a crucial role in the stabilization and coverage of nanoparticles. In addition to their involvement in the synthesis process, these phytochemicals can act as surfactants, ensuring the desired morphology and stability of the nanoparticles. Furthermore, they can influence the properties of the nanoparticles, such as their antibacterial or anticancer activities. Fourier-transform infrared spectroscopy (FTIR) and energy-dispersive X-ray spectroscopy (EDX) were employed to analyze the functional groups, proteins, and other components in the extract, before and after nanoparticle synthesis. These techniques provide valuable insights into the chemical composition and elemental analysis.

The intense and unusual peak observed at 3424 cm^{-1} in the FTIR spectrum of anatase nanoparticles corresponds to the stretching vibrations of OH groups. Additional peaks of stretching vibrations at 2924 cm^{-1} (C = C/O), 1634 cm^{-1} (C-H)[18,89], and 1283 cm^{-1} (N-O) suggest contributions from various functional groups. A weak peak at 2370 cm^{-1} is attributed to C ≡ C/N stretching vibrations[90]. The strong peak at 530 cm^{-1} corresponds to the Ti-O bond, typical for metal-oxygen bonds in the 400–800 cm^{-1} range. A previous study on spinach extract for iron oxide nanoparticle synthesis exhibited a similar FTIR spectrum, suggesting potential similarities in organic components. This technique provided qualitative evidence of the presence of carbon, nitrogen, titanium, and oxygen atoms in the synthesized nanoparticles[53].

The EDX of nanoparticles confirms the presence of titanium and oxygen atoms at a high percentage, which provides evidence for the construction of these nanoparticles. Detecting sub-atoms such as carbon, nitrogen, and even oxygen further supports the presence of organic compounds on the surface of the nanoparticles. In a study involving the synthesis of anatase phase nanoparticles using S. rosmarinus leaf extract, the EDX analysis demonstrated the presence of carbon and oxygen atoms on the surface of hemispherical nanoparticles. It was suggested that these atoms are likely associated with the organic substances present in the extract and act as stabilizers[17]. Spinach is accepted as a valuable source of iron. The presence of iron atoms is representative of spinach. The absence of sulfur atoms shows no impurity from the precursor salt in the final product due to centrifuging and washing.

Sample characterization yielded positive results, prompting an investigation into the nanoparticles' antimicrobial properties. Conventional methods like disc and well diffusion placement were unsuitable due to challenges in binding the effective substance at the desired concentration to the disc and the deposition of nanoparticles in the wells. To address these issues without chemical stabilizers for TiO_2 aggregation[91], a broth micro-dilution test was adopted, a method used in previous studies by R. Ahmad et al.[92], S. Vembu et al.[75], and A. Chatterjee et al.[93].

Quantitative analysis of absorbance at 600 nm, following a 24-hour incubation period, revealed that anatase nanoparticles (which are light inactive) exhibited a minimum inhibitory concentration of 0.5 mg/ml against E. coli and 2 mg/ml against S. aureus. The results indicate that the nanoparticles were more effective against E. coli. Interestingly, the antibacterial activity of the nanoparticles demonstrated favorable results even with no UV radiation, as observed in the experiment conducted in the dark. A similar study involving the synthesis of

anatase nanoparticles using C. nocturnum leaf extract also exhibited good antibacterial activity in the absence of light[94].

The absence of light suggests a mechanical disruption mechanism for the nanoparticles' antibacterial action. Gram-negative bacteria, with their less robust cell walls than gram-positive counterparts, are typically more susceptible to this type of disruption[72,88,95]. To date, no bacterial resistance to nanoparticles has been reported, likely due to their physical mode of action. Provided bacteria do not develop resistance to physical damage, nanoparticles could become a valuable alternative to antibiotics. This study supports the antimicrobial efficacy of titanium nanoparticles reported by other researchers.

Conclusion:

This study presents a novel, straightforward, and biocompatible methodology for titanium dioxide nanoparticle fabrication by reducing $TiOSO_4$ utilizing the aqueous extract derived from spinach leaves. Titanium dioxide nanoparticle synthesis was optimized by carefully adjusting temperature, concentration, and extract volume. Our findings indicate that using spinach leaf extract with a thickness ratio of 1/30, a 20 ml volume, and 200 µl of salt at a temperature of 50 degrees Celsius and a pH of 8 results in the formation of anatase-phase titanium dioxide nanoparticles. Nanoparticles' morphological, chemical, and structural characteristics were meticulously examined using various analytical techniques. The deliberate choice of the anatase phase is pivotal due to its exceptional photocatalytic properties, which hold significant relevance across diverse applications. Furthermore, we conducted an antibacterial assay on Bacillus cereus and Escherichia coli bacteria, yielding favorable results that underscore the potential of these green-synthesized nanoparticles. These results may prove that green synthesis nanoparticles, with easy production and favorable characteristics, can find their place in medicine and industry. To unlock their full potential, further research into these nanoparticles could pave the way for innovative and effective systems in future applications. Previous research demonstrated several applications across fields such as biomedicine, drug delivery, agriculture, and environmental science. However, our emphasis on biological approaches, antibacterial properties, and other unique features adds a fresh perspective to this burgeoning field.

Data availability

"The datasets used and/or analysed during the current study available from the corresponding author on reasonable request."

Received: 29 June 2024; Accepted: 16 September 2024
Published online: 28 September 2024

References

1. Santhoshkumar, T. et al. Green synthesis of titanium dioxide nanoparticles using Psidium guajava extract and its antibacterial and antioxidant properties. *Asian Pac. J. Trop. Med.* **7**, 968–976 (2014).
2. Akinola, P. O. et al. Multifunctional titanium dioxide nanoparticles biofabricated via phytosynthetic route using extracts of Cola nitida: Antimicrobial, dye degradation, antioxidant and anticoagulant activities. *Heliyon* **6** (2020).
3. Komaraiah, D., Madhukar, P., Vijayakumar, Y., Reddy, M. V. R. & Sayanna, R. Photocatalytic degradation study of methylene blue by brookite TiO_2 thin film under visible light irradiation. *Mater. Today Proc.* **3**, 3770–3778 (2016).
4. Mohamad, M. et al. A density functional study of structural, electronic and optical properties of titanium dioxide: Characterization of rutile, anatase and brookite polymorphs. *Mater. Sci. Semicond. Process.* **31**, 405–414 (2015).
5. Chavali, M. S. & Nikolova, M. P. Metal oxide nanoparticles and their applications in nanotechnology. *SN Appl. Sci.* **1**, 607 (2019).
6. Zhang, J., Zhou, P., Liu, J. & Yu, J. New understanding of the difference of photocatalytic activity among anatase, rutile and brookite TiO_2. *Phys. Chem. Chem. Phys.* **16**, 20382–20386 (2014).
7. Leal, J. H., Cantu, Y., Gonzalez, D. F. & Parsons, J. G. Brookite and anatase nanomaterial polymorphs of TiO_2 synthesized from TiCl3. *Inorg. Chem. Commun.* **84**, 28–32 (2017).
8. Sun, Y., Wang, S. & Zheng, J. Biosynthesis of TiO_2 nanoparticles and their application for treatment of brain injury-an in-vitro toxicity study towards central nervous system. *J. Photochem. Photobiol B* **194**, 1–5 (2019).
9. Arabi, N., Kianvash, A., Hajalilou, A., Abouzari-Lotf, E. & Abbasi-Chianeh, V. A facile and green synthetic approach toward fabrication of alcea-and thyme-stabilized TiO_2 nanoparticles for photocatalytic applications. *Arab. J. Chem.* **13**, 2132–2141 (2020).
10. Harlapur, S. F. et al. Photocatalytic studies of TiO_2 nanomaterials prepared via facile wet chemical route. *Mater. Today Proc.* **4**, 11713–11719 (2017).
11. Žerjav, G., Žižek, K., Zavašnik, J. & Pintar, A. Brookite vs. rutile vs. anatase: Whats behind their various photocatalytic activities? *J. Environ. Chem. Eng.* **10**, 107722 (2022).
12. Szołdra, P. et al. Effect of brookite on the photocatalytic properties of mixed-phase TiO_2 obtained at a higher temperature. *Mater. Sci. Engineering: B* **287**, 116104 (2023).
13. El-Zohry, A. M., Kloo, L. & He, L. Understanding charge dynamics in TiO_2 using ultrafast mid-infrared spectroscopy: Trapping versus recombination. *J. Phys. Chem. C* (2024).
14. Kondo, H., Machmudah, S., Kanda, H., Zhao, Y. & Goto, M. Synthesis of titanium dioxide nanoparticle by means of discharge plasma over an aqueous solution under high-pressure gas environment. *Alexand. Eng. J.* **61**, 3805–3820 (2022).
15. Ahmed, Y., Hussain, J. & Asif, S. Green synthesis of copper oxide and cobalt oxide nanoparticles using spinacia oleracea leaf extract.
16. Pakseresht, S., Cetinkaya, T., Al-Ogaili, A. W. M., Halebi, M. & Akbulut, H. Biologically synthesized TiO_2 nanoparticles and their application as lithium-air battery cathodes. *Ceram. Int.* **47**, 3994–4005 (2021).
17. Silva-Osuna, E. R., Vilchis-Nestor, A. R., Villarreal-Sanchez, R. C., Castro-Beltran, A. & Luque, P. A. Study of the optical properties of TiO_2 semiconductor nanoparticles synthesized using *Salvia rosmarinus* and its effect on photocatalytic activity. *Opt. Mater. (Amst)* **124**, 112039 (2022).
18. Moriyama, A., Yamada, I., Takahashi, J. & Iwahashi, H. Oxidative stress caused by TiO_2 nanoparticles under UV irradiation is due to UV irradiation not through nanoparticles. *Chem. Biol. Interact.* **294**, 144–150 (2018).
19. Ebrahimi, K., Shiravand, S. & Mahmoudvand, H. Biosynthesis of copper nanoparticles using aqueous extract of *Capparis spinosa* fruit and investigation of its antibacterial activity. *Marmara Pharm. J.* **21**, 866–871 (2017).
20. Monson, T. C., Rodriguez, M. A., Leger, J. L., Stevens, T. E. & Huber, D. L. A simple low-cost synthesis of brookite TiO_2 nanoparticles. *J. Mater. Res.* **28**, 348–353 (2013).

21. Souri, M., Hoseinpour, V., Ghaemi, N. & Shakeri, A. Procedure optimization for green synthesis of manganese dioxide nanoparticles by *Yucca gloriosa* leaf extract. *Int. Nano Lett.* **9**, 73–81 (2019).
22. Salam, H. A. & Sivaraj, R. *Ocimum basilicum* L. var. purpurascens Benth.-LAMIACEAE mediated green synthesis and characterization of titanium dioxide nanoparticles. *Adv. Biores* **5** (2014).
23. Kaur, K. & Thombre, R. Nanobiotechnology Methods, applications, and future prospects. In *Nanobiotechnology* 1–20 (Elsevier, 2021).
24. Fakruddin, M., Hossain, Z. & Afroz, H. Prospects and applications of nanobiotechnology: A medical perspective. *J. Nanobiotechnol.* **10**, 1–8 (2012).
25. Diniz, S. N., Sosnik, A., Mu, H., Valduga, C. J. & Nanobiotechnology *BioMed Res. Int.* vol. Preprint at (2013) (2013).
26. Singh, K. R. B., Nayak, V., Singh, J., Singh, R. L. & Singh, R. P. Introduction: Nanobiotechnology for the livestock industry. In *Nanobiotechnology for the Livestock Industry* 1–27 (Elsevier, 2023).
27. Qamar, S. A., Asgher, M., Khalid, N. & Sadaf, M. Nanobiotechnology in health sciences: Current applications and future perspectives. *Biocatal. Agric. Biotechnol.* **22**, 101388 (2019).
28. Hussain, I., Singh, N. B., Singh, A., Singh, H. & Singh, S. C. Green synthesis of nanoparticles and its potential application. *Biotechnol. Lett.* **38**, 545–560 (2016).
29. Tyagi, P. K. et al. Green synthesis of iron nanoparticles from spinach leaf and banana peel aqueous extracts and evaluation of antibacterial potential. *J. Nanomater.* 1–11 (2021).
30. Lakshmi, S. J. et al. Biosynthesis and characterization of ZnO nanoparticles from spinach (*Spinacia oleracea*) leaves and its effect on seed quality parameters of greengram (*Vigna radiata*). *Int. J. Curr. Microbiol. App Sci.* **6**, 3376–3384 (2017).
31. Ashraf, H. et al. Antifungal potential of green synthesized magnetite nanoparticles black coffee–magnetite nanoparticles against wilt infection by ameliorating enzymatic activity and gene expression in *Solanum lycopersicum* L. *Front. Microbiol.* **13**, 754292 (2022).
32. Djouadi, A. & Derouiche, S. Spinach mediated synthesis of zinc oxide nanoparticles: Characterization, in vitro biological activities study and in vivo acute toxicity evaluation. *Curr. Res. Green. Sustainable Chem.* **4**, 100214 (2021).
33. Verma, V. et al. A Review on green synthesis of TiO_2 NPs: Synthesis and Applications in photocatalysis and antimicrobial. *Polymers* **14**, 1444. Preprint at (2022) (2022).
34. Hussain, S. et al. Green synthesis of TiO_2 nanoparticle in Morus nigra leaves; characterization and biological potential. *Pol. J. Environ. Stud.* **33** (2024).
35. Doğan, B., Yeşilyurt, M. K., Yaman, H., Korkmaz, N. & Arslan, A. Green synthesis of SiO_2 and TiO_2 nanoparticles using safflower (*Carthamus tinctorius* L.) leaves and investigation of their usability as alternative fuel additives for diesel-safflower oil biodiesel blends. *Fuel* **367**, 131498 (2024).
36. Jayan, N. & Metta, L. D. B. Process optimization by response surface methodology-central composite design for the adsorption of lead by green synthesized TiO_2 using *Phyllanthus acidus* extract. *Biomass Convers. Biorefin* **14**, 825–845 (2024).
37. Kondala Rao, T. A study of green synthesis of nano TiO_2 catalyst by gossypium leaf extract and its nanocatalysis in the synthesis of bio fuel from gossypium seed oil. *Nano Life* (2024).
38. Mbenga, Y., Adeyemi, J. O., Mthiyane, D. M. N., Singh, M. & Onwudiwe, D. C. Green synthesis, antioxidant and anticancer activities of TiO_2 nanoparticles using aqueous extract of *Tulbhagia violacea*. *Results Chem.* **6**, 101007 (2023).
39. Pavithra, S. et al. Photocatalytic and photovoltaic applications of green synthesized titanium oxide (TiO_2) nanoparticles by *Calotropis gigantea* extract. *J. Alloys Compd.* **960**, 170638 (2023).
40. Abdulrazaq, H. A. & Alwared, A. I. Bio-synthesis of TiO_2 using grape leaves extract and its application for photocatalytic degradation of ibuprofen from aqueous solution. *Environ. Technol.* 1–13 (2023).
41. Asmat-Campos, D., Rojas, M. L. & Carreño-Ortega, A. Toward sustainable nanomaterials: An innovative ecological approach for biogenic synthesis of TiO_2 nanoparticles with potential photocatalytic activity. *Clean. Eng. Technol.* **17**, 100702 (2023).
42. Pillai, A. M. et al. Bio-synthesized TiO_2 nanoparticles and the aqueous binder-based anode derived thereof for lithium-ion cells. *Discover Nano* **19**, 1–14 (2024).
43. Rahmawati, D. et al. Synthesis of TiO_2 nanoparticles using red spinach leaf extract (Amaranthus Tricolor L.) for photocatalytic of methylene blue degradation. *Green. Chem. Lett. Rev.* **17**, 2352571 (2024).
44. Pandya, S. Estimation of iron and copper from spinach leaves.
45. Jakhrani, M. A. et al. Biogenic preparation of ZnO nanostructures using leafy spinach extract for high-performance photodegradation of methylene blue under the illumination of natural sunlight. *Molecules* **28**, 2773 (2023).
46. Kisan, B., Shruthi, H., Sharanagouda, H., Revanappa, S. B. & Pramod, N. K. Effect of nano-zinc oxide on the leaf physical and nutritional quality of spinach. *Agrotechnology* **5**, 135 (2015).
47. Thandapani, G. et al. Green synthesis of copper oxide nanoparticles using Spinacia oleracea leaf extract and evaluation of biological applications: Antioxidant, antibacterial, larvicidal and biosafety assay. *Mater. Today Commun.* **34**, 105248 (2023).
48. Al-Jawhari, H., Bin-Thiyab, H. & Elbialy, N. In vitro antioxidant and anticancer activities of cupric oxide nanoparticles synthesized using spinach leaves extract. *Nano-Structures Nano-Objects* **29**, 100815 (2022).
49. Azmat, R., Altaf, I. & Moin, S. The reflection of the photocatalytic properties of TiO_2 nanoparticles on photosynthetic activity of *Spinacia oleracea* plants. *Pak J. Bot.* **52**, 1229–1234 (2020).
50. Ahmadi-Nouraldinvand, F., Afrouz, M., Tseng, T. M. P., Poshtdar, A. & Coudret, C. Green synthesis of hyperbranched spermine-coated Fe_3O_4 nanoparticles and their effect on corn seedlings under copper oxide stress. *ACS Sustain. Chem. Eng.* **11**, 12888–12907 (2023).
51. Jha, V. C. & Mishra, R. Biosynthesis of Iron nanoparticles from *Spinacia oleracea* and its application in wastewater treatment. *Migration Lett.* **20**, 19–26 (2023).
52. Shammeri, A., Abu-Huwaij, R. & Hamed, R. Development and characterization of magnetic hydrogels loaded with greenly synthesized iron-oxide nanoparticles conjugated with cisplatin. *Pharm. Dev. Technol.* **29**, 383–392 (2024).
53. Fayyaz, B., Zahra, M. B. & Haider, M. S. Screening of phenolic compounds from spinach (*Spinacia oleracea*), green synthesis of iron-nanoparticles and determination of its anti-microbial effect on *Escherichia coli*. (2022).
54. Al-Zaqri, N. et al. Photocatalytic degradation of rhodamine B and methylene blue using novel Spinacia oleracea-based Ag nanoparticles: Experimental and theoretical analysis. *Eur. Phys. J. Plus* **138**, 958 (2023).
55. Shnain, S. M. & Habeebalshamsi, H. A. Biological synthesis of copper oxide nanoparticles using spinach extract. *Int. J. Pharm. Res.* **09752366**, 12 (2020).
56. Stanić, V. & Tanasković, S. B. Antibacterial activity of metal oxide nanoparticles. in *Nanotoxicity* 241–274 (Elsevier, 2020).
57. Sunny, N. E. et al. Green synthesis of titanium dioxide nanoparticles using plant biomass and their applications—a review. *Chemosphere* **300**, 134612 (2022).
58. Brabazon, D. & Raffer, A. Chapter 3—advanced characterization techniques for nanostructures. In *Emerging Nanotechnologies for Manufacturing* (eds. Ahmed, W. & Jackson, M. J.) 59–91 (William Andrew Publishing, Boston, 2010). https://doi.org/10.1016/B978-0-8155-1583-8.00003-X
59. Wei, X., Liu, Y., El-kott, A., Ahmed, A. E. & Khames, A. Calendula officinalis-based green synthesis of titanium nanoparticle: Fabrication, characterization, and evaluation of human colorectal carcinoma. *J. Saudi Chem. Soc.* **25**, 101343 (2021).
60. Shahin Lefteh, M., Sourinejad, I. & Ghasemi, Z. Biosynthesis of Titanium Dioxide nanoparticles from the Mangrove (Avicennia marina) and investigation of its antibacterial activity. *J. Mazandaran Univ. Med. Sci.* **30**, 15–27 (2020).

61. Velayutham, K. et al. Evaluation of *Catharanthus roseus* leaf extract-mediated biosynthesis of titanium dioxide nanoparticles against *Hippobosca maculata* and *Bovicola ovis*. *Parasitol. Res.* **111**, 2329–2337 (2012).
62. Amanulla, A. M. & Sundaram, R. Green synthesis of TiO_2 nanoparticles using orange peel extract for antibacterial, cytotoxicity and humidity sensor applications. *Mater. Today Proc.* **8**, 323–331 (2019).
63. Rajendhiran, R., Deivasigamani, V., Palanisamy, J., Masan, S. & Pitchaiya, S. *Terminalia catappa* and *Carissa carandas* assisted synthesis of TiO_2 nanoparticles—a green synthesis approach. *Mater. Today Proc.* **45**, 2232–2238 (2021).
64. Aravind, M., Amalanathan, M. & Mary, M. S. M. Synthesis of TiO_2 nanoparticles by chemical and green synthesis methods and their multifaceted properties. *SN Appl. Sci.* **3**, 1–10 (2021).
65. Rajakumar, G. et al. Solanum trilobatum extract-mediated synthesis of titanium dioxide nanoparticles to control *Pediculus humanus* capitis, *Hyalomma anatolicum* anatolicum and *Anopheles subpictus*. *Parasitol. Res.* **113**, 469–479 (2014).
66. Rajakumar, G. et al. Efficacy of larvicidal activity of green synthesized titanium dioxide nanoparticles using *Mangifera indica* extract against blood-feeding parasites. *Parasitol. Res.* **114**, 571–581 (2015).
67. Gandhi, P. R., Jayaseelan, C., Vimalkumar, E. & Mary, R. R. Larvicidal and pediculicidal activity of synthesized TiO_2 nanoparticles using *Vitex negundo* leaf extract against blood feeding parasites. *J. Asia Pac. Entomol.* **19**, 1089–1094 (2016).
68. Amina, M., Al Musayeib, N. M., Alarfaj, N. A., El-Tohamy, M. F. & Al-Hamoud, G. A. Antibacterial and Anticancer Potentials of Presynthesized Photosensitive Plectranthus cylindraceus Oil/TiO_2/Polyethylene Glycol Polymeric Bionanocomposite. *Bioinorg. Chem. Appl* 5562206 (2021).
69. Subhapriya, S. & Gomathipriya, P. Green synthesis of titanium dioxide (TiO_2) nanoparticles by *Trigonella foenum*-graecum extract and its antimicrobial properties. *Microb. Pathog* **116**, 215–220 (2018).
70. Jafari, A., Rashidipour, M., Kamarehi, B., Alipour, S. & Ghaderpoori, M. Toxicity of green synthesized TiO_2 nanoparticles (TiO_2 NPs) on zebra fish. *Environ. Res.* **212**, 113542 (2022).
71. Solano, R. A., De León, L. D., De Ávila, G. & Herrera, A. P. Polycyclic aromatic hydrocarbons (PAHs) adsorption from aqueous solution using chitosan beads modified with thiourea, TiO_2 and Fe3O4 nanoparticles. *Environ. Technol. Innov.* **21**, 101378 (2021).
72. Punitha, V. N., Vijayakumar, S., Sakthivel, B. & Praseetha, P. K. Protection of neuronal cell lines, antimicrobial and photocatalytic behaviours of eco-friendly TiO_2 nanoparticles. *J. Environ. Chem. Eng.* **8**, 104343 (2020).
73. Victor, W. S. et al. Biogenesis of TiO_2 nanoparticles: An approach to prove multidisciplinary application. *Green. Synthesis Catal.* **3**, 150–155 (2022).
74. Narayanan, M. et al. Synthesis and characterization of TiO_2 NPs by aqueous leaf extract of *Coleus aromaticus* and assess their antibacterial, larvicidal, and anticancer potential. *Environ. Res.* **200**, 111335 (2021).
75. Vembu, S., Vijayakumar, S., Nilavukkarasi, M., Vidhya, E. & Punitha, V. N. Phytosynthesis of TiO_2 nanoparticles in diverse applications: What is the exact mechanism of action? *Sens. Int.* **3**, 100161 (2022).
76. Achudhan, D. et al. The antibacterial, antibiofilm, antifogging and mosquitocidal activities of titanium dioxide (TiO_2) nanoparticles green-synthesized using multiple plants extracts. *J. Environ. Chem. Eng.* **8**, 104521 (2020).
77. Win, H. Y. Y., Oo, N. S. W. & Chin, K. M. Analysis on Phytochemicals, Minerals and Total Flavonoid Content of Spinach (Spinacia oleracea Linn.). in (2020).
78. Bellavite, P. Neuroprotective potentials of flavonoids: Experimental studies and mechanisms of action. *Antioxidants* **12**, 280 (2023).
79. Solovchenko, A. & Solovchenko, A. Screening pigments: General questions. *Photoprotection Plants: Opt. Screening-based Mech.* 9–31 (2010).
80. Bunea, A. et al. Total and individual carotenoids and phenolic acids content in fresh, refrigerated and processed spinach (*Spinacia oleracea* L.). *Food Chem.* **108**, 649–656 (2008).
81. Doak, J., Gupta, R. K., Manivannan, K., Ghosh, K. & Kahol, P. K. Effect of particle size distributions on absorbance spectra of gold nanoparticles. *Phys. E Low Dimens Syst. Nanostruct.* **42**, 1605–1609 (2010).
82. Sethy, N. K., Arif, Z., Mishra, P. K. & Kumar, P. Green synthesis of TiO_2 nanoparticles from *Syzygium cumini* extract for photo-catalytic removal of lead (pb) in explosive industrial wastewater. *Green. Process. Synthesis* **9**, 171–181 (2020).
83. Morelock, T. E. & Correll, J. C. Spinach. In *Vegetables I: Asteraceae, brassicaceae, Chenopodicaceae, and cucurbitaceae* 189–218 (Springer, 2008).
84. Balaji, S. et al. Green synthesis of nano-titania (TiO_2 NPs) utilizing aqueous *Eucalyptus globulus* leaf extract: Applications in the synthesis of 4 H-pyran derivatives. *Res. Chem. Intermed.* **47**, 3919–3931 (2021).
85. Soni, N. & Dhiman, R. C. Larvicidal and antibacterial activity of aqueous leaf extract of Peepal (*Ficus religiosa*) synthesized nanoparticles. *Parasite Epidemiol. Control* **11**, e00166 (2020).
86. Srinivasan, M. et al. Green synthesis and characterization of titanium dioxide nanoparticles (TiO_2 NPs) using *Sesbania grandiflora* and evaluation of toxicity in zebrafish embryos. *Process Biochem.* **80**, 197–202 (2019).
87. Reddy, P. N. K. et al. Structural, optical and electrochemical properties of TiO_2 nanoparticles synthesized using medicinal plant leaf extract. *Ceram. Int.* **45**, 16251–16260 (2019).
88. Ramya, S. et al. TiO_2 nanoparticles derived from egg shell waste: Eco synthesis, characterization, biological and photocatalytic applications. *Environ. Res.* **214**, 113829 (2022).
89. scholar.
90. Goutam, S. P. et al. Green synthesis of TiO_2 nanoparticles using leaf extract of *Jatropha curcas* L. for photocatalytic degradation of tannery wastewater. *Chem. Eng. J.* **336**, 386–396 (2018).
91. Domingos, R. F., Tufenkji, N. & Wilkinson, K. J. Aggregation of titanium dioxide nanoparticles: Role of a fulvic acid. *Environ. Sci. Technol.* **43**, 1282–1286 (2009).
92. Ahmad, R., Mohsin, M., Ahmad, T. & Sardar, M. Alpha amylase assisted synthesis of TiO_2 nanoparticles: Structural characterization and application as antibacterial agents. *J. Hazard. Mater.* **283**, 171–177 (2015).
93. Chatterjee, A., Ajantha, M., Talekar, A., Revathy, N. & Abraham, J. Biosynthesis, antimicrobial and cytotoxic effects of titanium dioxide nanoparticles using *Vigna unguiculata* seeds. *Int. J. Pharmacognosy Phytochemical Res.* **9**, 95–99 (2017).
94. Tahir, K. et al. Visible light photo catalytic inactivation of bacteria and photo degradation of methylene blue with Ag/TiO_2 nanocomposite prepared by a novel method. *J. Photochem. Photobiol B* **162**, 189–198 (2016).
95. Kiwi, J., Rtimi, S., Sanjines, R. & Pulgarin, C. TiO_2 and TiO_2-doped films able to kill bacteria by contact: New evidence for the dynamics of bacterial inactivation in the dark and under light irradiation. *Int.J. Photoenergy* (2014).

Acknowledgements

We would like to thank the research council of Tarbiat Modares University for their financial support through this investigation.

Author contributions

F.SH: Data curation, Formal analysis, Investigation, Methodology, Visualization, Writing - original draft. S.D: Data curation, Formal analysis, Investigation, Methodology, Project administration, Supervision, Validation, Visualization, Funding acquisition, Writing - review & editing.

Declarations

Competing interests
The authors declare no competing interests.

Additional information
Correspondence and requests for materials should be addressed to S.D.

Reprints and permissions information is available at www.nature.com/reprints.

Publisher's note Springer Nature remains neutral with regard to jurisdictional claims in published maps and institutional affiliations.